Journal of Nanoscience and Nanotechnology
Vol. 5, 2050–2056, 2005

Adsorption of a Microtubule on a Charged Surface Affects its Disassembly Dynamics

Yi Yang,[1] R. Guzman,[2] P. A. Deymier,[1,*] M. Umnov,[3] J. Hoying,[4]
S. Raghavan,[1] O. Palusinski,[3] and B. J. J. Zelinski[1]

[1] *Department of Materials Science and Engineering,* [2] *Department of Chemical and Environmental Engineering,*
[3] *Department of Electrical and Computer Engineering, and* [4] *Biomedical Engineering Program,*
Nano-Biomolecular Engineering Science and Technology (n-BEST) Program, The University of Arizona, Tucson AZ 85721, USA

The dynamics of disassembly of microtubules deposited on surfaces is shown to be strongly dependent on the electrostatic interaction between the microtubule and the substrate. Fluorescence microscopy of microtubules adsorbed on a Poly-L-Lysine film and immersed in pure water show a drastic decrease in disassembly velocity compared to the microtubules in bulk water solutions. While microtubules suspended in pure water disassemble in seconds, the dissociation velocity of microtubules adsorbed on a Poly-L-Lysine film ranges from 0.8 to 1.0 μm/min in pure water. Kinetic Monte Carlo simulations of the microtubule dynamics indicate that a decrease in the dissociation velocity of unstable microtubules can be achieved by reducing the heterodimer dissociation rate constant of tubulin heterodimers constituting a single protofilament, adsorbed to the Poly-L-Lysine film. This model suggests that the reduction of the dissociation velocity originates from the electrostatic interactions between the positively charged amino groups of the Poly-L-Lysine film and the negatively charged microtubule surface.

Keywords: Microtubule Dynamics, Disassembly, Poly-L-Lysine, Charged Surface, Monte Carlo Simulation, Interconnects, Bottom-Up.

1. INTRODUCTION

In recent years, the exponential growth in semiconductor technology has been sustained by extending the capabilities of top-down manufacturing processes based on lithography to shorter and shorter wavelengths. Unfortunately, the costs of these top-down approaches are projected to be prohibitive at sizes and tolerances in the nanometer range. In response, a new paradigm has arisen based on the bottom-up or molecular engineering approach to the mass replication of nanoscale electronic circuits that promises to be cheaper, more flexible, and efficient. Control of interconnections emerges as one of the major challenges in the development of these bottom-up approaches. Current state of knowledge suggests that biomolecules and assemblies of biomolecules may offer the control necessary for inexpensive and reliable fabrication of nanoscale interconnects.

Protein-based nano-structures with large aspect ratio and nanoscale diameter, such as microtubules (MT) have been considered as templates for the fabrication of electrically conductive nanowires.[1] Microtubules are naturally formed proteinaceous nano-tubes, 24 nm in diameter and up to hundreds of microns in length. MTs are biopolymers assembled from two related protein monomers: α and β tubulins.[2] In the presence of the small molecule guanosine 5′-triphosphate (GTP), these tubulin monomers form a heterodimer, which self-assemble into the microtubule structure. Metallization of MTs for improving their electrical conduction has been achieved via electroless plating methods.[1]

Due to the geometry of self-assembly and differences in addition rates, a MT is polarized containing (−) and (+) ends. The (−) end contains exposed α tubulins and undergoes slower heterodimer addition rates than the (+) end, which consists of exposed β tubulins. Therefore, net MT polymerization occurs from the (+) end of the

*Author to whom correspondence should be addressed.

 1533-4880/2005/5/2050/007 doi:10.1166/jnn.2005.510

growing polymer or nucleation complex. MTs generated from pure tubulins exist in a dynamic state with net addition of monomers to the (+) end and net removal of monomers from the (−) end.[3] Dynamic instability is an intrinsic property of MTs.[4] For $\alpha\beta$-tubulin concentration above a critical value C_c, tubulin dimers polymerize into MTs; while below C_c, MTs depolymerize.[2] Near C_c, MTs exhibit dynamic instability during which a single MT undergoes apparently random successive periods of assembly (slow growth) and disassembly (rapid depolymerization). The ability to control MT polymerization states offers a significant advantage in the fabrication of templates for metallic nanowires and interconnects over more traditional approaches in which material addition is irreversible. However, electroless plating baths for metallization of MTs exhibit harsh chemistries that promote MT disassembly. MTs have been stabilized prior to metallization by crosslinking the tubulin subunits with dialdehyde.[5] Several proteins, called microtubule-associated proteins (MAPs) have MT-binding activity and play important roles in MT polymerization and regulation, including the stabilization of polymerized MTs.[6] Recently, we have shown that MAPs play a critical role in maintaining the MT stability during Pt-catalyzed electroless Ni plating.[7] MAP-stabilized MTs metallized for one minute in a Ni-acetate-based electroless-plating bath were coated with a metal film several nanometers thick.[7] MAPs do not suppress the MT dynamics nearly as much as dialdehyde but still allow control of the MT disassembly process.

Biomolecules immobilized on surfaces behave differently than in solution. Such immobilization renders the biomolecules unique characteristics and properties including a certain degree of increased molecular stability towards different factors such as pH and ionic strength variations. Many immobilization strategies have been developed and used to study protein adsorption phenomena. These include chemisorption as well as physisorption on organic and inorganic supports. Physisorption of proteins on glass or organic matrices coated with polymeric materials such as polylysine, dialdehyde, and nitrocellulose have been widely used. In fact, spotted microarrays of nucleic acids and proteins are mostly based on this type of physical adsorption.[8] In order to produce MT templates on a silica substrate for the fabrication of nanowires with specific length and orientation, the assembly and disassembly processes of MTs on this very substrate must be controlled. The fixation of biological substances on a silica substrate by covalent crosslinking using, for instance, dialdehyde is irreversible and therefore inappropriate for MTs as they could not disassemble afterward. MTs also can adhere strongly to the amine terminal silane surfaces, while retaining their biological activity.[9] AFM microscopy measurements of disassembly of MTs electrostatically or covalently bound on surfaces show large fluctuations in their disassembly rate.[10] Poly-L-Lysine (PLL) polymers spontaneously adsorb from aqueous solution onto glass or silicon dioxide surfaces that are negatively charged with its polycationic PLL backbone strongly interacting with such surfaces.[11–14] MTs can be immobilized and stabilized through electrostatic interactions with the positively charged amino groups of the PLL film bound to the negatively charged glass or silicon surfaces.

The development of MTs-based interconnect technology necessitates compatibility with commonly used microelectronics chemical environments. In this paper we show that (a) MAP-rich MTs are unstable in microelectronic grade ultra pure water, (b) the disassembly dynamics in ultra pure water of MTs deposited on PLL films coated silicon dioxide substrates (glass or thermal oxide on silicon wafer) is reduced, and (c) the slower MT disassembly is due to a smaller dissociation rate of the tubulin heterodimers adsorbed on the PLL film that may result from the electrostatic interaction between the negatively charged heterodimers and the positively charged PLL film.

In Section 2 we present the experimental methods and measurements of time for complete dissociation of free MTs and MTs adsorbed on PLL films in ultra pure water. A kinetic Monte Carlo model that accounts for a lower dissociation rate of heterodimers adsorbed on the PLL film is used to simulate the dynamic instability of MTs attached onto the PLL modified substrate. The model and the results of simulations are given in Section 3. The experimental and the simulation results are compared and discussed in Section 4.

2. EXPERIMENTAL APPROACH AND RESULTS

In this work, we used MAP-rich tubulin (∼30% MAPs). The tubulin was prepared from bovine brain extracts (Cytoskeleton Inc.), and was stored at −70 °C in G-PEM buffer [pH 6.8; 80 mM Piperazine-N, *N*′-bis [2-ethanesulfonic acid sequisodium salt (PIPES), 1 mM Magnesium chloride ($MgCl_2$); 1 mM Ethylene glycol-bis(b-amino-ethyl ether) *N*,*N*,*N*′,*N*′-tetra-acetic acid (EGTA) and 1 mM Guanosine 5′-triphosphate (GTP)]. *In-vitro* MT assembly was performed in PEM 80 buffer (80 mM PIPES, 1 mM EGTA, 4 mM $MgCl_2$, using KOH to adjust the pH to 6.9) with a final concentration of tubulin of 1.5 mg/ml. Polymerization was performed by the addition of GTP (final concentration is 0.25 mM) and Taxol (∼20 μM). The final solution was rotated at 15 rpm for 30 min at 37 °C for polymerization. Then, the solution was centrifuged at 14500 g for 30 minutes to separate MTs from the unpolymerized tubulin. The supernatant was removed and about 5-fold volume of fresh PEMTAX solution (20 μM Taxol+PEM80 buffer) was added to resuspend the MTs. One microliter MAP stabilized MTs stock solution was diluted in 50 microliters PEMTAX solution.

RESEARCH ARTICLE

The graft poly-L-Lysine (PLL) copolymers were spontaneously adsorbed from dilute aqueous solution onto negatively charged surfaces such as glass and metal oxide surfaces (including silicon oxides, titanium oxides and niobium oxides). In the field of biology, poly-L-Lysine coated glass slides are frequently used to attach cells and tissues. In our research, glass slides coated with a PLL film were prepared as follows. The slides were immersed in a mixture of 600 μL of PLL solution (Sigma Diagnostics Inc., PLL, 0.1% w/v in water with thimerosal, 0.01%, added as a preservative) and 300 ml of ethanol for 20 min, and then dried at 60 °C. Wafers coated with PLL were considered good only for 3 days after coating. We deposited a small drop of the diluted MTs solution onto the Poly(L-Lysine) coated slide and we let it stand for 30 minutes for MTs to sediment onto the slide surface. The slide was then rinsed in double distilled water for 0, 1, 5, and 10 minutes.

During our experiments, the surface coatings of the PLL on the glass surface were similar to results reported in the literature for coatings with 1 mg/ml bulk solutions of PLL formulations.[15–17] Values reported for similar derivatives are around 180 ng/cm^2.[15] In our experimental protocols we used approximately 3 cm^2 of coated surface. The amount of PLL adsorbed on the glass surface would be roughly 540 ng. This value corresponds to approximately 2.7×10^{-6} micromoles of PLL and at least 10^4 times larger than the amount of moles of MTs in solution. Thus we expected to have enough PLL adsorbed on the surface to immobilize effectively MTs from solution.

MTs were visualized by fluorescence immuno-labeling using a monoclonal antibody (in PBS buffer) directed against β tubulin as the primary antibody (anti-β-tubulin, clone TUB 2.1, Sigma Inc.) Prepared MTs were fixed with Methanol at −20 °C for 3 minutes and incubated with the primary antibody for 30 min at room temperature. A secondary goat antibody conjugated with Cy3 and directed against mouse IgG (Sigma Inc.,) was mixed with the primary antibody-labeled MT for 30 min. PBS buffer (Phosphate buffered saline, pH 7.4) was used for all washing steps.

We conducted a series of experiments to investigate the stability of MTs both suspended in pure water and adsorbed on PLL coated glass slides. Our other experiments showed that MTs are stable in PEM80 buffer solution with the presence of 20 μm taxol, even at very low concentrations. However, when suspended in pure water, MTs are unstable. Experiments have been conducted to investigate the stability of MAP-enriched, Taxol-stabilized MTs in pure water. At first, polymerized MTs with an average length of 10 microns were diluted into 50-fold volume of pure water. The concentration of MTs was measured as a function of time using optical adsorption with a wavelength of 340 nm. After several seconds of suspension in pure water, the concentration of MTs dropped to nearly undetectable level. In contrast, the disassembly of

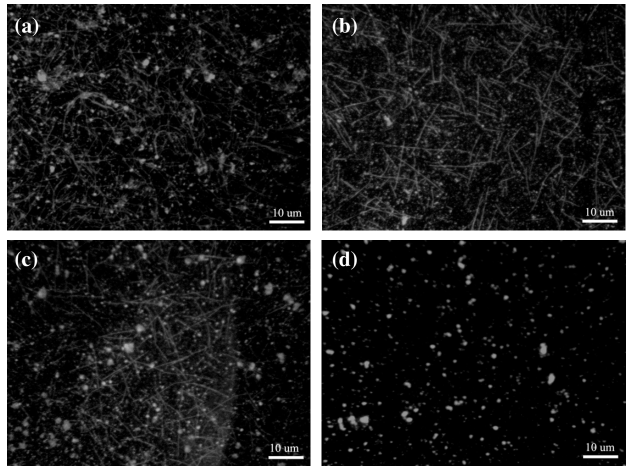

Fig. 1. Fluorescence microscopy pictures of MTs adsorbed on glass slides coated with a Poly(L-Lysine) film immersed in pure water for (a) 0 min, (b) 1 min, (c) 5 min, (d) 10 min. Immersion in pure water for 10 min yielded a surface free of MTs.

the MTs adsorbed on PLL coated glass slides, following immersion in pure water, is slowed down. This observation is illustrated in Figure 1(b) and (c), where the number of MTs per unit area slightly decreases after 1 and 5 min of immersion in water, compared to that of the control experiment (Fig. 1(a)). After being immersed in water for 10 min (Fig. 1(d)), all surface-adsorbed MTs were gone. The reproducibility of the results of Figure 1(a–d) has been verified by conducting three series of experiments. The MT length distributions normalized to the fraction of surviving adsorbed MTs are plotted in Figure 2. The distributions of lengths are determined from an analysis of the images of three sets of experiments similar to Figure 1.

We have superimposed the initial distribution (time = 0) translated by −1.0 μm and −3.5 μm on the distributions at 1 min and 5 min parts, respectively. This superposition clearly illustrates the nearly uniform shortening of the MTs with a disassembly rate in the interval [0.8, 1.0] μm/min. At this time we have to make a distinction between MT depolymerization and simple detachment of MTs from the coated substrate. Detachment cannot be ruled out as participating in the reduction of the MT surface density with time. However, on the ground of weaker electrostatic interactions, short MTs could be expected to detach more easily. Since distributions of Figure 2 are not skewed toward the longer MTs as time evolves, one concludes that there is little detachment from the substrate or that the rate of detachment is independent of MT length and that the normalized distributions are consequently representative of the disassembly of MTs.

In addition to the disassembly on coated glass slides we have considered other substrates. We also report on the dissociation of MT adsorbed on substrates constituted of 4 mm × 4 mm oxidized silicon chips with gold electrodes patterned on the layer of thermal silicon dioxide. The oxide layer is approximately 500 nm thick. The gold

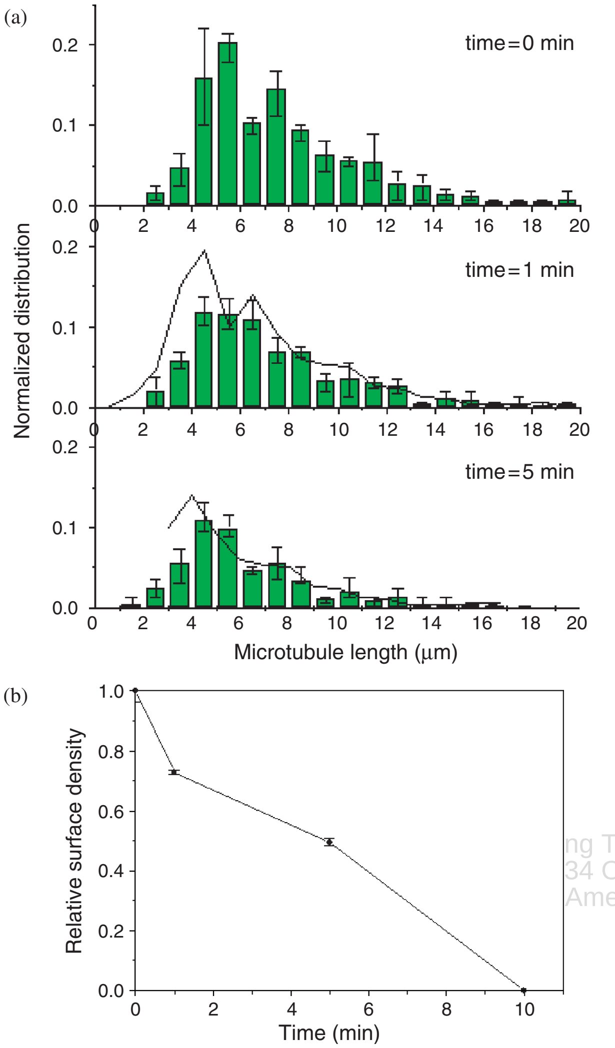

Fig. 2. (a) MT length distributions at three subsequent times of immersion in water average over three sets of experiments. The distributions are normalized to the MT surface density. The solid lines superimposed on the 1 and 5 min distributions are the envelopes of the initial distribution translated by -1.0 μm and -3.5 μm, respectively. (b) Presents the ratio of the surface density of MTs to the initial surface density as a function of immersion time in pure water. Surface density is determined by counting the number of microtubules per area on fluorescence microscopy images. Lengths of microtubules are measured directly from these images.

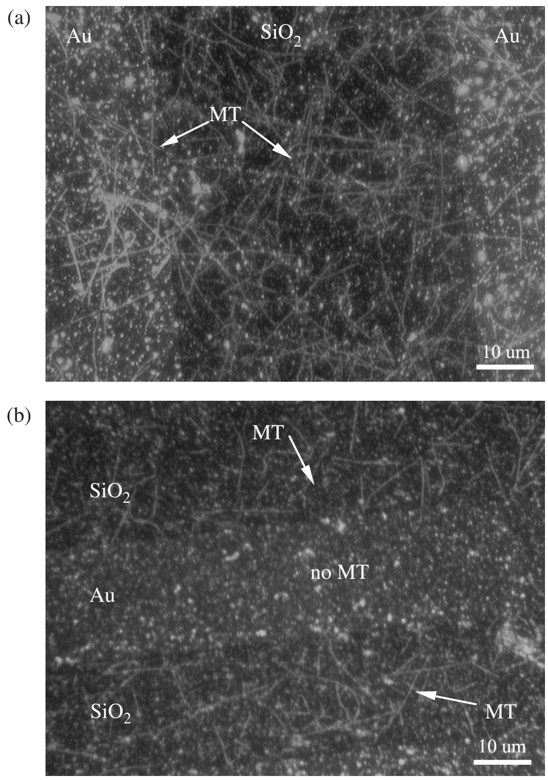

Fig. 3. Fluorescence microscopy pictures of MTs deposited on a patterned silicon wafer coated with Poly(L-Lysine) and immersed for (a) 0 min (left and right regions are gold electrodes) and (b) 3 min (central region is gold electrode).

electrodes rise above the silicon dioxide with a measured step height ranging from 65 to 95 nm. The patterned silicon wafers were coated with a PLL film following the same protocol as for the glass slides. PLL does not bind naturally to gold. To attach PLL to gold substrate, one would have to use a self-assembled monolayer of the alkanethiol mercaptoundecanoic acid (MUA) to coat the gold first, then PLL is electrostatically adsorbed onto the monolayer.[18] Deposition of MT on the coated wafers was also done in the same way. The wafers were rinsed in pure water for 3 min and MTs were visualized using fluorescence microscopy. In absence of immersion in pure water, MTs could be found evenly distributed on the gold electrodes as well as the PLL coated oxidized wafer (see Fig. 3(a)). Since PLL does not bind to gold, immersion in water leads to rapid disassembly or detachment of the MTs settled on the gold electrodes and slow disassembly of the MTs bound to the PLL film. In Figure 3(b), microtubules are not found on the gold electrodes (central region). Figure 3(b) also shows unambiguously that the MTs bound to the PLL coated silica substrate have not completely disassembled and consequently that their dissociation dynamics was slowed down. In Figure 4, we illustrate the chemical structure and the charge distribution of the PLL film on a silicon dioxide substrate as well as the association of the PLL film with a MT. An evaluation of the electrostatic properties of a MT, based on the recent solution of the structure of tubulin,[19] showed an overall negative electrostatic potential of the MT with smaller regions of positive potential.[20] A negatively charged MT will therefore attach electrostatically to the positively charged amino groups exposed at the end of the side-chain of the PLL molecules. The side-chain of lysine has an unusually high pKa value (10.53) for an amino group and consequently is positively charged even in moderate alkaline media. Heterodimers electrostatically bound to the film are expected to possess a reduced dissociation rate constant leading to slower disassembly dynamics. To verify this hypothesis, we show in Section 3 with

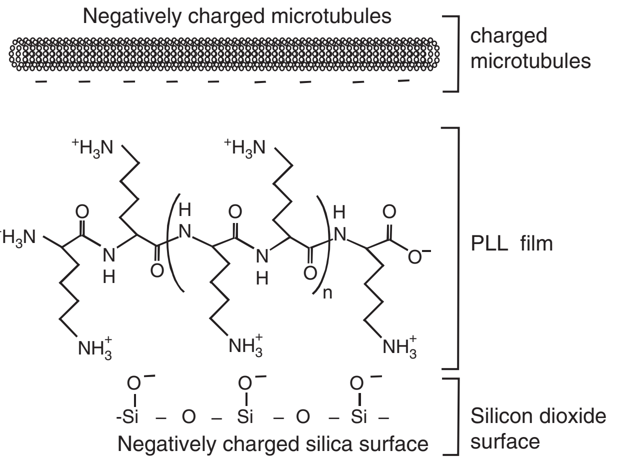

Fig. 4. Illustration of the chemical structure of Poly(L-Lysine) molecules on a silicon dioxide substrate and charge distribution of the MT-PLL-SiO_2 assembly.

a computer simulation that a reduction of the dissociation rate of only some tubulin heterodimers (i.e., these heterodimers constituting a single protofilament in direct contact with and bound to the PLL film) drastically impacts the overall dissociation velocity of a MT.

3. COMPUTER MODEL AND SIMULATION RESULTS

Computer simulations of MT assembly/disassembly have recreated many experimentally observed aspects of MT behavior and have given strong support to a cap model of MT dynamics. There exists several cap models but since the nature of the cap is unknown, modeling MT dynamics requires the choice of a particular capping model. Here we use the GTP lateral cap model to investigate the effect of adsorption of MT dynamics. This model utilizes a coarse grained representation of the protein tubulin heterodimers and supposes that growing MTs are stabilized by a cap of tubulin dimers that have GTP molecules associated with the β-tubulin monomer.

Early kinetic MC studies of models based on simplified single-helix[21] and multihelices[22] generated phase change between a slow-growing GTP capped MT end and rapidly shortening uncapped MT end. Subsequent simulations by Bailey et al.[23,24] were based on a simplified helical lattice model with only longitudinal and single lateral interactions between $\alpha\beta$-tubulin subunits (the "lateral cap model"). Bailey's model differs from the model of Chen and Hill[22] in that it gives a molecular description to the switching of MT between assembling and disassembling states in terms of a fully coupled mechanism linking Tubulin-GTP (Tu-GTP) addition and GTP hydrolysis (conversion of Tu bound GTP into the di-phosphate GDP). Bailey's model focused on the "5-start" helical 13-protofilament MT lattice. MTs are known to readily form different lattices, some having a "seam" in which the lateral interactions between adjacent protofilaments are misaligned.[25] Martin et al.[26] have developed a more rigorous lattice model that accounts for MT lattice variations and seams. In this latter model, association and dissociation rate-constants are obtained from estimates of the free energies of specific protein–protein interactions in terms of the basic MT lattice. The performance of kinetic MC simulations of MTs does not appear to be too sensitive to the detailed numerical values assigned to the intersubunit bond energies.[27] Martin's model rationalizes the dynamic properties in terms of a metastable MT lattice of Tu-GDP stabilized by the kinetic process of Tu-GTP addition. Furthermore, with this model, the effects of small tubulin-binding molecules are readily treated. The lateral cap model provides a basis for the examination of the effect of antimitotic drugs (e.g., colchicine, Taxol) on MT dynamics. In particular, it was used to study the control of MT dynamics by substoichiometric concentration of drugs. The lateral cap model was further modified to simulate the effect of MT assembly/disassembly on transport of a motor protein-coated bead that moves along a protofilament.[28]

Here we implement a modified version of the five-start helix lattice model of Bailey.[23] With this model a single MT consists of a two-dimensional helical lattice composed of 13 grid sites (13 tubulin heterodimer protofilaments) perpendicular to the direction of growth (MT principal axis) (see Fig. 5). The lattice is infinite along the principal direction of the MT. Helical periodic boundary conditions (PBC) are applied to wrap the lattice into a tubular structure with a helicity of five lattice points (i.e., sites A and A′ in Fig. 5 are contiguous). Assembly/disassembly is limited to one end of the model effectively neglecting the contribution of the slowest end of the MT to its dynamics. The main difference between Bailey's model and ours is that the heterodimers in protofilament 6 (black squares in Fig. 5) are hypothesized to adsorb onto the PLL film and will be assigned a reduced dissociation rate (see Step 2

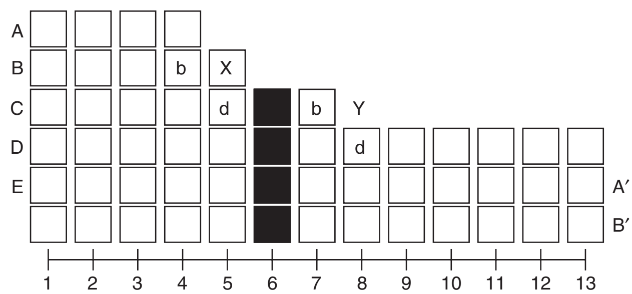

Fig. 5. Schematic illustration of the arrangement of heterodimers at the end of a microtubule with 13-protofilaments. Site A′ is contiguous to site A because of helical periodic boundary conditions. X and Y are dissociation and association sites respectively. The sites b and d, adjacent to X or Y, determine the value of the dissociation or association constants. The black squares represent the heterodimers in protofilament adsorbed onto a Poly(L-Lysine) film.

below). This is consistent with the experimental observation of disassembling MTs adsorbed to surfaces, leaving behind protofilaments on the surface.[10]

The steps involved in the kinetic MC simulation of MT dynamics at fixed tubulin-GTP concentration ([Tu-GTP]) are as follows:

Step 1: We identify at the ends of each protofilament along the jagged helical surface of the tip of a MT) the sites "i" for dissociation (occupied grid site at the top of a step i.e., site X) and association (empty grid site A the bottom of a step i.e., site Y).

Step 2: We assign a rate constant k_i for dissociation or association events at every site "i". These rate constants depend on the physical structure of the binding site, the nucleotide content of the unit in adjacent protofilaments (i.e., both relate to the binding free energy) and [Tu-GTP] in the case of association. We use the association and dissociation rate constants of the standard set of Bayley et al.[23,24] For the sake of simplicity, we consider only the dependence of the rate constants on the nature of the heterodimers at site "b" and "d" adjacent to sites X or Y (Fig. 5). To account for the binding interaction between the adsorbed heterodimers and the PLL film, the dissociation rate constant of heterodimers in protofilament 6 is modified by a multiplying factor, $F \leq 1$.

Step 3: We calculate the time t_i for dissociation or association at every site "i" at which an event would occur statistically, using the relationship $t_i = -\ln(1-R_i)/k_i$, where R_i is a random number uniformly distributed between 0 and 1.

Step 4: The event with the shortest time ($t_{\min}$) is accepted and the lattice is modified. For addition events, we implement a hydrolysis rule for conversion of Tu-GTP into Tu-GDP when a Tu-GTP molecule is completely embedded into the MT lattice.

Step 5: The total time is incremented by $t_{\min}$.

Step 6: The simulation stops when the MT is completely dissociated or has grown to a length of 2000 heterodimers.

The initial MT length is 500 $\alpha\beta$ tubulin heterodimers or 4 μm. For each concentration of Tu-GTP and each reducing factor, F, we run a series of a minimum of 10 simulations with different random numbers. Below C_c, the MT disassembles and the negative growth rate (disassembly rate) is calculated as minus the initial length divided by the time for complete dissociation. The calculated growth and disassembling rates are in reasonable agreement with experimentally determined growth and shortening velocities of individual MT.[29] Above C_c, the growth rate is determined from the time it takes the MT to grow to a length of 16 μm (i.e., 2000 heterodimers). The average growth rate versus Tu-GTP concentration is reported in Figure 6 for four values of F, namely 1, 0.1, 0.01, and 0.001. The concentration at which the growth rate changes sign is the critical concentration C_c. The critical concentration decreases to lower values as the binding of a single protofilament to the PLL film increases, that is, when F decreases.

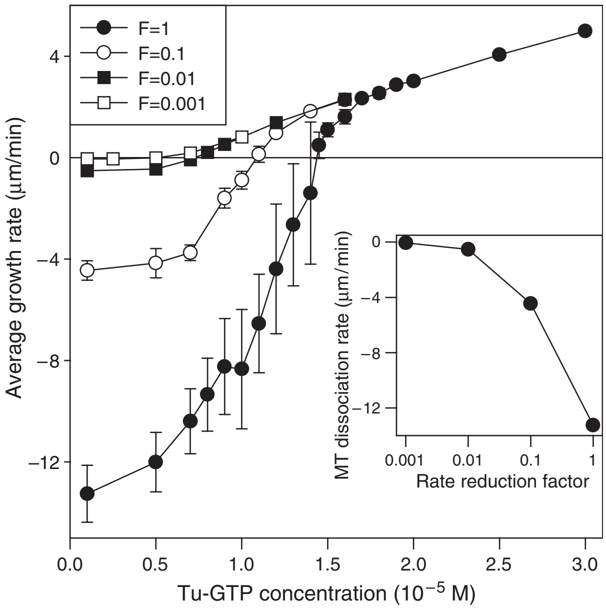

Fig. 6. Calculated average growth rate of a MT adsorbed onto a Poly(L-Lysine) film versus Tu-GTP concentration. The closed circles, open circles, close squares, and open squares correspond to a reduction by a factor, F, of 1, 0.1, 0.01, and 0.001 of the dissociation rate constant for heterodimers in the 6th protofilament. The inset reports dissociation rates in pure water ([Tu-GTP]) ~0) as a function of F.

The factor, F, does not affect the association rate constants at high Tu-GTP concentration. All curves converge to the same asymptote. In our experiments, MTs were diluted into pure water, which has no Tu-GTP present (or a very low concentration of Tu-GTP when some MTs disassembled). Thus they should be on the left half of Figure 6. The growth rate at very low Tu-GTP concentration (approaching pure water in the limit of $[\text{Tu-GTP}] = 0$) as a function of F is represented in the inset. This inset shows that the binding between a surface and a single protofilament has a very high impact on the disassembly dynamics of a MT. In absence of binding to the substrate ($F = 1$), the dissociation rate exceeds -13 μm/min indicating that a 4 μm long microtubule would dissociate in pure water within less than 20 seconds. On the other hand a 4 μm MT bound to a PLL film with a dissociation rate reduction factor of 0.01 would take more than 7 min to completely dissociate in pure water. This model shows that disassembly dynamics of MTs is drastically altered by reducing the dissociation rate constant of only one of its protofilaments. This reduction in rate constant may arise from interaction between substrate and the heterodimers in contact with that substrate.

Our model does not account for the possibility of a change in structure of the end of disassembling MT such as its break up into curved protofilaments.[30] In that case, we still expect that splaying of individual protofilaments would be inhibited or strongly perturbed by the adsorption of a MT onto a surface. In addition, considering the elastically stabilized structural cap models,[31]

RESEARCH ARTICLE

attachment of Tu-GDP protofilaments to a flat surface will affect their tendency to form curved configurations and stabilize MTs.

4. CONCLUSIONS

We have shown experimentally and theoretically that the binding electrostatic interaction between tubulin heterodimers constituting MTs and a Poly(L-Lysine) film reduced significantly the kinetics of dissociation of MTs in pure water. MTs are unstable in pure water,[29] but adsorbing them on a positively charged substrate can control their disassembly velocity. We find experimentally that the dissociation velocity of MTs adsorbed on a PLL film ranges from 1 to 2 μm/min. Kinetic Monte Carlo simulations of MT dynamics indicate that a decrease in the dissociation velocity of unstable MTs can be achieved by reducing the heterodimer dissociation rate constant of tubulin heterodimers constituting a single protofilament, namely the protofilament adsorbed to the positively charged amino groups of the PLL film. The dissociation velocity estimated from experiments can be explained with a reduction of the adsorbed-heterodimer dissociation rate constant by a factor of 1/50 to 1/20.

Finally, it is worth noting that an experimental study of the dynamic instability of individual MAP-free MT clean glass substrate showed no significant interaction between the glass surface and the MT.[29] In that particular case the glass surface is negatively charged and in such conditions it would not have any adsorption effect on the attachment of the negatively charged MTs. In contrast, the present study stresses the effect of MT/substrate interactions on MT dynamics when the substrate is coated with a PLL film exposing positive charges.

Acknowledgments: We would like to acknowledge financial support from the National Science Foundation, grant # 0303863. This work was supported in part by a small research grant from the office of the Vice President for Research at the University of Arizona and the University of Arizona Foundation. We would like to acknowledge additional financial support from the College of Engineering and Mines and the department of Materials Science and Engineering at the University of Arizona. We would like to acknowledge assistance of Victor Wells and Sarah Dahl of the University of Arizona's Microelectronics Laboratory in fabrication of suitable silicon substrates.

References and Notes

1. R. Kirsch, M. Mertig, W. Pompe, R. Wahl, K. J. Bohm, E. Unger, and G. Sadowski, *Thin Solid Films* 305, 248 (**1997**).
2. H. Lodish, A. Berk, S. L. Zipursky, P. Matsudaira, D. Baltimore, and J. E. Darnell, *Molecular Cell Biology*, Freeman, New York (**2000**), 4th edn.
3. S. C. Schuyler and D. Pellman, *Cell* 105, 421 (**2001**).
4. T. Mitchison and M. Kirschner, *Nature* 312, 232, 237 (**1984**).
5. S. Behrens, K. Rahn, N. Habicht, K. J. Bohm, H. Rosner, E. Dinjus, and E. Unger, *Adv. Mater.* 14, 1621 (**2002**).
6. K. Kinoshita, I. Arnal, A. Desai, D. N. Drechsel, and A. A. Hyman, *Science* 294, 1340 (**2001**).
7. Y. Yang, B. H. Constance, P. A. Deymier, J. Hoying, S. Raghavan, and B. J. J. Zelinski, *J. Mater. Sci.* 39, 1927 (**2004**).
8. M. Schena, D. Shalon, R. W. Davis, and P. O. Brown, *Science* 270, 467 (**1995**).
9. D. C. Turner, C. Chang, K. Fang, S. L. Brandow, and D. B. Murphy, *Biophys. J.* 69, 2782 (**1995**).
10. N. H. Thomson, S. Kasas, B. M. Riederer, S. Catsicas, G. Dietler, A. J. Kulik, and L. Forro, *Ultramicroscopy* 97, 239 (**2003**).
11. G. L. Kenausis, J. Voros, D. L. Elbert, N. P. Huang, R. Hofer, L. Ruiz-Taylor, M. Textor, J. A. Hubbell, and N. D. Spencer, *J. Phys. Chem. B* 104, 3298 (**2000**).
12. D. L. Elbert and J. A. Hubbell, *Chem. Biol.* 5, 177 (**1998**).
13. L. A. Ruiz-Taylor, T. L. Martin, F. G. Zaugg, K. Witte, P. Indermuhle, S. Nock, and P. Wagner, *Proc. Natl. Acad. Sci. USA* 98, 852 (**2001**).
14. S. Faraasen, J. Voros, G. Csucs, M. Textor, H. P. Merkle, and E. Walter, *Pharm. Res.* 20, 237 (**2003**).
15. S. VandeVondele, J. Voros, and J. A. Hubbell, *Biotech. Bioengr.* 82, 784 (**2003**).
16. R. Taylor, T. L. Martin, F. G. Zaugg, K. Witte, P. Indermuhle, S. Nock, and P. Wagner, *PNAS* 98, 852 (**2001**).
17. E. Haber, L. B. Page, and G. A. Jacoby, *Biochem.* 4, 693 (**1965**).
18. B. L. Frey, C. E. Jordan, S. Kornguth, and R. M. Corn, *Anal. Chem.* 67, 4452 (**1995**).
19. E. Nogales, M. Whittaker, R. A. Milligan, and K. H. Downing, *Cell* 96, 79 (**1999**).
20. N. A. Baker, D. Dept, S. Joseph, M. J. Holst, and J. A. McCammon, *PNAS* 98, 10037 (**2001**).
21. T. L. Hill and Y. Chen, *Proc. Natl. Acad. Sci. USA* 81, 5772 (**1984**).
22. Y. Chen and T. L. Hill, *Proc. Natl. Acad. Sci. USA* 82, 1131 (**1985**).
23. P. Bayley, M. Schilstra, and S. Martin, *FEBS Letts.* 259, 181 (**1989**).
24. P. M. Bayley, M. J. Schilstra, and S. R. Martin, *J. Cell. Sci.* 95, 33 (**1990**).
25. E. M. Mandelkow, R. Schultheiss, R. Rapp, M. Muller, and E. Mandelkow, *J. Cell. Biol.* 102, 1067 (**1986**).
26. S. R. Martin, M. J. Schilstra, and P. M. Bayley, *Biophys. J.* 65, 578 (**1993**).
27. R. A. B. Keater, Dynamic microtubule simulation, seams and all. *Biophys. J.* 65, 566 (**1993**).
28. Y. Tao and C. S. Peskin, *Biophys. J.* 75, 1529 (**1998**).
29. D. K. Fygenson, E. Braun, and A. Libchaber, *Phys. Rev. E* 50, 1579 (**1994**).
30. I. Arnal, E. Karsenti, and A. Hyman, *J. Cell Biology* 149, 767 (**2000**).
31. I. M. Janosi, D. Chretien, and H. Flyvbjerg, *Biophys. J.* 83, 1317 (**2002**).

Received: 18 June 2004. Revised/Accepted: 19 November 2004.

RESEARCH ARTICLE